Journal Name

Dynamic Article Links ►

Cite this: DOI: 10.1039/c0xx00000x

www.rsc.org/xxxxxx

ARTICLE TYPE

Identification of TiO_2 nanoparticles using La and Ce as labels. Application to the evaluation of surface contamination during the handling of nano-sized matter

Virginia Gómez,[a] Alberto Clemente,[a] Silvia Irusta,[a,b]* Francisco Balas[a,b] and Jesus Santamaria[a,b]*

Received (in XXX, XXX) Xth XXXXXXXXX 20XX, Accepted Xth XXXXXXXXX 20XX
DOI: 10.1039/b000000x

Distinguishing nanomaterials of interest from background nanosized matter already present in the sampling environment is a challenging task. In this work we propose the use of Rare Earth Elements (REE) as high-sensitivity labels to identify and to monitor their fate following manipulation. The REE labels were added during the synthesis of TiO_2 nanoparticles with hydrodynamic sizes of 15 nm. The REE-labelled nanomaterials allow the monitoring of nanoparticle aerosols caused during handling of nanoparticulate material in a glove box. The deposition of the labelled TiO_2 nanoparticles on working surfaces could be verified by electron microscopy and surface analysis, using the presence of lanthanide elements as an identification label. The total amount of TiO_2 nanoparticles in the deposited material could be quantified by a procedure based in wiping the deposition area followed by digestion of the collected matter and analysis by flame emission spectrometry.

Introduction

Airborne nanosized matter is ubiquitous in the air we breathe, not only in research [1] and industrial locations,[2] but also in natural environments.[3, 4] Nanoparticles may also be generated in the context of common daily life activities, such as soldering or using metal utensils.[5, 6] However, in recent years we have witnessed a growing interest regarding the possibility of adverse effects of nanomaterials in human health.[7, 8] Of especial concern are the so-called engineered nanomaterials (ENMs), new synthetic nanomaterials to which there has been scant or no previous exposure. Indeed, many toxicity studies are underway using ENMs [9-11] under carefully controlled laboratory conditions. For instance, Abid et al.,[12] used europium-doped gadolinium oxide nanoparticles to study the deposition, clearance and translocation of nanoparticles in a mouse lung. However, in any real life exposure assessment, the concentration of the ENMs under consideration will have to be determined, which is a challenging task.[13] The main difficulty is related to the fact that the proportion of ENMs in relation to background nanosized matter is likely to be extremely low (in the ppm range or lower), and therefore direct observation by usual techniques such as electron microscopy can generally be ruled out as a method to quantify exposure. Hence, alternative means of identification and discrimination of ENMs are needed. One possibility is labelling the ENMs using specific tags that are not present in the sampling environment. A variety of labelling techniques have been used, which generally involve granting additional, specific properties to the target nanomaterials (Table 1). Some authors have used labelled nanoparticles to avoid interferences during the assessment of toxicity to specific nanomaterials.[14-18] Also, fluorescent dyes,[19-21] radioactive tracers [22-24] or stable isotopes [25, 26] have been used to trace nanoparticles under several conditions. Other identification techniques exploit the enhanced properties of the matter at the nanoscale, such as the catalytic properties of some types of nanomaterials.[27, 28] The selection of a label must take into account the application scenario, i.e., the label should not interfere with the aspect to be studied. In this respect, the modification of the substrates by different markers may lead to different behaviour of the nanomaterials (see for instance [25]). Moreover, some labelling methods, such as radioactive labelling raise concerns upon disposal and waste treatment, and may require expensive facilities for performing the labelling and identification procedures.

In this work we have used REE (La and Ce ions) to label TiO_2 nanoparticles. In order to include the REE in the nanoparticle structure and to minimize the impact on relevant properties (such as particle size distribution, surface charge, specific area and pore structure) we have used a modified sol-gel procedure in which the REE addition is integrated in the synthesis process. TiO_2 was selected in view of its wide range of applications, which increases the potential for unintended release and exposure [29] and also because of the enormous variety of commercial presentations and functionalizations.[13] The inclusion of lanthanide ions, namely cerium and lanthanum, in REE/Ti ratios up to 0.03 could be effectively traced using analytical and microscopic techniques under different conditions. As a proof of concept of the use of

Table 1. Reported nanoparticle labelling and identification methods

Material	Labelling/Identification	Analysis Technique	Reference
TiO_2 NPs	Radiolabelling: Proton irradiation with a cyclotron [a)]	--------	[30]
Several ENMs	Radiolabelling: Ion-beam or neutron irradiation [a)]	---------	[31]
Ag, Co/Co_3O_4, and CeO_2	Radiolabelling: Neutron activation	γ-ray spectrometry	[18]
ZnO	Stable isotope [a)]	ICP-MS	[16]
ZnO	Stable isotope [a)]	CARS, STEM-EDX, MC-ICP-MS	[19]
Pt, Ni, Pd, Fe_2O_3 ENPs	Catalytic [b)]	SMPS, BET and TEM. Catalytic FTIR	[20]
Pd and Ni	Catalytic [b)]	CAAM	[21,22]
Carboxyl-modified polystyrene	Fluorescence	Confocal microscopy and Flow cytometry	[13]
Carbon nanofibers CNFs.	Non-labelled [a)]	Thermal-optical analysis for carbon	[24a]

[a] Offline

[b] Online

REE labelling, the contamination of work surfaces by labelled TiO_2 nanoparticles after manipulation in the laboratory was quantitatively assessed. Pouring powder between two beakers was used because it has been addressed as a potential source for emission of nanoparticles in laboratory environments, [32] and it is a very usual laboratory operation.

Experimental

Synthesis of REE-labelled TiO_2 nanoparticles

The synthesis process has been described elsewhere[33]. Briefly, 2 mL of titanium (IV) isopropoxide (Sigma-Aldrich, 97%) and 30 ml of ethanol (EtOH, Panreac, analytical grade) were mixed under magnetic stirring. An amount of 3 mL of acetic acid (AcOH, Panreac) was added after 5 min. Samples with REE/Ti atomic ratios of 0, 0.005, 0.01 and 0.03 have been obtained by adding the stoichiometric amounts of cerium (III) nitrate ($Ce(NO_3)_3 \cdot 6\ H_2O$) and lanthanum (III) nitrate ($La(NO_3)_3 \cdot 6\ H_2O$) to the solution under stirring. After 5 min, 5 mL of deionized water was added and the mixture was poured into an autoclave, which was sealed and heated up to 120ºC for 15 min in a microwave oven (Ethos Plus). The final solid powder was isolated by centrifugation, thoroughly washed with EtOH several times and dried at 80ºC for 24 h.

Characterization of REE-labelled TiO_2 nanoparticles

The size, morphology, composition and distribution of lanthanides in the TiO_2 nanoparticles were analysed by means of scanning electron microscopy coupled with energy dispersive X-ray analysis (SEM-EDX, FEI-F Inspect and INCA PentaFETX3) and transmission electron microscopy (TEM, Tecnai T20). Statistical size-distribution histograms were obtained from TEM images using Image J software ($N > 75$). The crystal structure, purity and crystal degree of the TiO_2 nanoparticles were determined using X-Ray Diffraction (XRD) in a Rygaku/Max System RU 300. UV-visible spectra of the samples were recorded in a Jasco V-670 spectrophotometer. The hydrodynamic nanoparticle size and ζ-potential in water were determined using dynamic light scattering (DLS) in a Brookhaven Instruments 90Plus. For the measurement of ζ-potential, phase analysis of light scattering (ZetaPALS) configuration was chosen, and 1-$mg \cdot mL^{-1}$ suspensions were prepared in milli-Q (Millipore) water. KOH or HNO_3 solutions were added to analyse the pH influence. The surface areas were measured by N_2 adsorption at 77 K in a Micromeritics TriStar analyser (Micromeritics, Norcross GA). Samples were outgassed at 26.7 Pa and 623 K for 6 h before performing adsorption experiments. Surface area was determined using the BET model applied to the range of relative pressures from 0.025 to 0.25. Mesopore size distributions were determined using the BJH data reduction scheme in the desorption branch of the isotherms. The chemical composition of REE-labelled TiO_2 nanoparticles was determined by inductively coupled plasma assisted optical emission spectroscopy (ICP-OES, ACTIVA-S Horiba-Jobin Yvon). The X-ray photoelectron analysis (XPS) was performed with an Axis Ultra DLD (Kratos Tech). The samples were mounted on a sample rod placed in the pretreatment chamber of the spectrometer and then evacuated at room temperature. The spectra were excited by the monochromatized AlKα source at 1486.6 eV and subsequently run at 12 kV and 10 mA. Survey spectrum was measured at 160 eV pass energy and for the individual peak regions, spectra were recorded with pass energy of 20 eV. The analysis of peaks was performed with the CasaXPS software, using a weighted sum of Lorentzian and Gaussian components curves after Shirley background subtraction. The binding energies were referenced to the internal C1s standard at 284.9 eV.

Monitoring of REE-TiO_2 nanoparticles during handling procedures

The experimental setup was located inside an acrylic glove box chamber (61x61x71 cm^3) that provides an isolated work environment. The relative humidity and temperature inside the chamber were measured during the experiments (30 - 45% RH and 22 - 25 ºC).

Two types of experiments were performed to monitor airborne particles and nanoparticle deposition during nanopowder manipulation. The transference of 500 mg of Ce-TiO_2 nanoparticles between two 100 mL beakers by gently pouring from one to another was used as potential contamination source.

During the first types of experiments, the particle emissions were studied by sampling the air around the beaker to measure the particle number concentration in the air with an Optical Particle Counter (OPC) from Grimm at 1.2 L/min. Besides, released airborne matter was sampled through TEM grids placed on a polycarbonate filter inside a 47-mm diameter stainless steel filter holder at a flow rate of 0.3 L/min. Morphology and shape of collected particles was observed and analysed by TEM and STEM-EDX using a Tecnai F30 microscope (FEI). In this case,

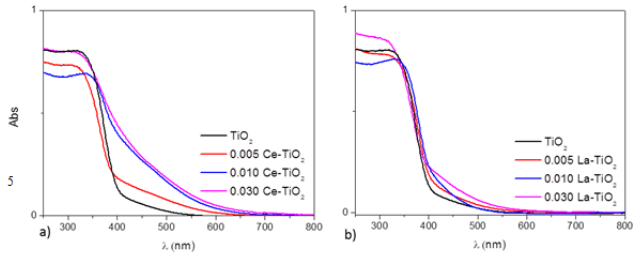

Fig. 1 UV/vis spectra of Ce-TiO_2 and La-TiO_2 nanoparticles.

the air of the chamber was purged with filtered clean air before the experiment to avoid the interference of ambient particles. The rest of the experiments were performed in the presence of ambient air.

On the other hand the nanoparticle deposition on the working surfaces of the glove box was studied. Specific identification as well as qualitative and quantitative measurements was performed. The glove box was thoroughly cleaned before each experiment and the same pouring process was carried out without gas phase sampling, to avoid disturbing the deposition process.

The deposition of airborne particles onto working area was qualitatively analysed after handling REE-labelled TiO_2 nanoparticulate powders in a delimited working surface (30x30 cm^2). In a first experiment four 1-cm^2 pieces of carbon tape were placed on the base of the handling chamber at 10 cm and 20 cm from the manipulation point. A mass of 500 mg of Ce-labelled TiO_2 powder was then poured once from a 100 mL glass beaker to another. Shape and morphology of the contamination particles settled on the surface tapes were carefully verified by using Scanning Electron Spectroscopy and Energy Dispersive X-ray Spectroscopy (FESEM, Inspect form FEI).

Quantitative analysis of the deposited nanoparticulate matter was performed according the OSHA standardized procedure (ID-125G) for sampling lead and other surface-deposited metals.[39] Briefly, sealed disposable wipes (Ghost Wipes made by cross linked polyvinyl alcohol, Reference 225-2414) was pre-moistened with deionized water and subsequently used for wiping the 30x30 cm^2 area in concentric squares of decreasing sizes while applying a firm pressure. This process was repeated twice after folding the wipe in half. Wipes were then dissolved in hot water and submitted to centrifugation at 10000 rpm during 5 min. The collected matter was further digested and analysed by ICP-OES to determine the concentration of Ce. A scheme of the method is shown in the Supporting Information file (Figure 2 S1). In order to test the efficiency of the procedure, a known amount of Ce-labelled TiO_2 nanoparticles were dispersed in water, deposited and allowed to dry in the testing surface. This process was repeated three times and the recovering percentage was estimated to be 75 ± 6 %.

Finally, three samples of the deposited particulated matter were collected from the 30 x 30 cm area after a handling process of 500 mg of cerium doped nanoparticles and its cerium content was subsequently analyzed.

Results and discussion

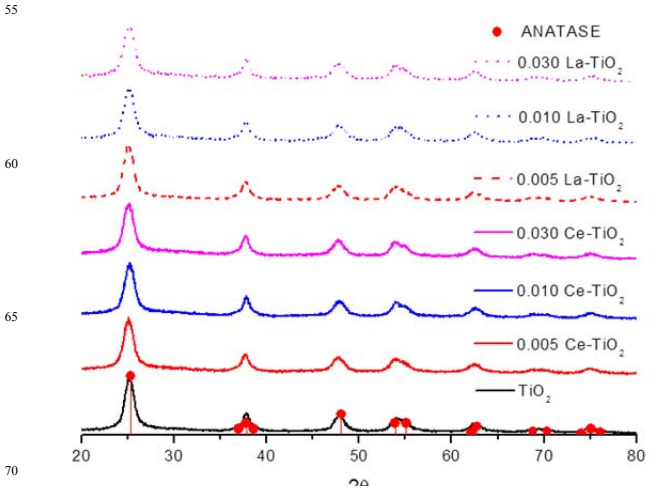

Fig.2 Powder XRD patterns of Ce-TiO_2 and La-TiO_2 nanoparticulate solids. (Red circles: position of anatase maxima)

Labelling and identification

The use of REE to label TiO_2 nanoparticles induced changes in their visual appearance. The addition of cerium during synthesis provoked a yellow colour on the solid, which is more intense as the nominal content of cerium increases.[34] This feature could be noticed as a shift to larger wavelengths in the visible absorption of samples for Ce-labelled TiO_2 (Figure 1). Similar behaviour was detected for La-labelled materials, though the effect was less marked. Incorporating metals in TiO_2 nanoparticles might affect the final properties of the material above a certain doping level. However, the high sensitivity of the technique developed means that the amount of added Ce and La needed for labelling is very low. Indeed, the amount of Ce and La added to the TiO_2 nanoparticles in this work was low enough to avoid any modification of the structural characteristics of the solids, and only a slight coloration could be noticed at the highest loadings. For most commercial applications, this slight coloration will not have any significant effect on the final colour of a material containing the labelled TiO_2 nanoparticles.

Structural analysis using XRD indicated that nanoparticles showed the tetragonal structure of anatase, regardless of the inclusion of lanthanide ions (Figure 2). Separate phases of the REE as CeO_2 or La_2O_3 could not be detected in the XRD patterns. The particle size of REE-labelled TiO_2 nanoparticles calculated using the Debye-Scherrer equation (Table 2) was very similar to that of unlabelled TiO2; only a small decrease (11-16%) could be noticed when REE ions were incorporated at the highest concentrations. This may be caused by the influence of REE ions on the growth of nanoparticles by affecting the hydration degree of the surface.[35]

Table 2. Structural parameters, surface area and REE/Ti and O/Ti atomic ratios calculated from Ln3d, Ti2p and O1s XPS signals for REE-labelled TiO_2 nanoparticles

Material	Nominal Ln/Ti ratio	Crystal grain size [nm][a)]	Surface area [$m^2 \cdot g^{-1}$] [b)]	O/Ti [c)]	REE/Ti [c)]
TiO_2	--	6.92	239	2.5	--
Ce_{05}-TiO_2	0.005	6.55	--	2.6	0.010
Ce_1-TiO_2	0.01	6.98	--	2.9	0.025
Ce_3-TiO_2	0.03	6.22	215	3.0	0.066
La_{05}-TiO_2	0.005	6.84	--	2.8	0.014
La_1-TiO_2	0.01	7.06	--	2.6	0.025
La_3-TiO_2	0.03	5.92	246	2.7	0.038

[a)] Estimated using the Debye-Scherrer equation for the XRD (101) maximum of the TiO_2 anatase structure.
[b)] Calculated using the BET procedure in the N_2 adsorption data at 77 K in the interval of relative pressures P/P_0 from 0.025 to 0.25
[c)] Calculated from XPS measurements

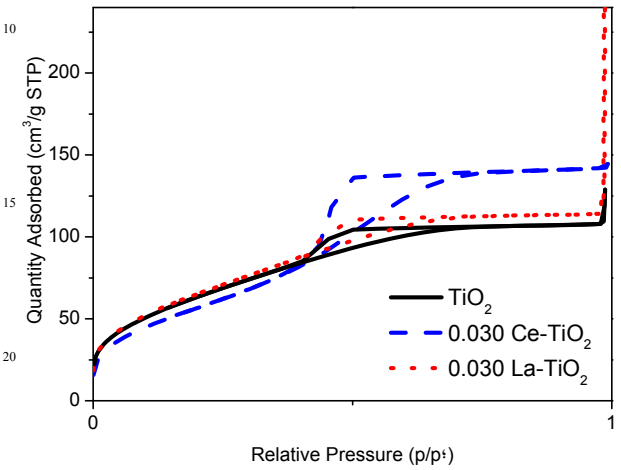

Fig. 3. Nitrogen adsorption–desorption isotherms at 77 K of Ce- and La-labelled TiO_2 nanoparticulate powders with a REE/Ti ratio of 0.03

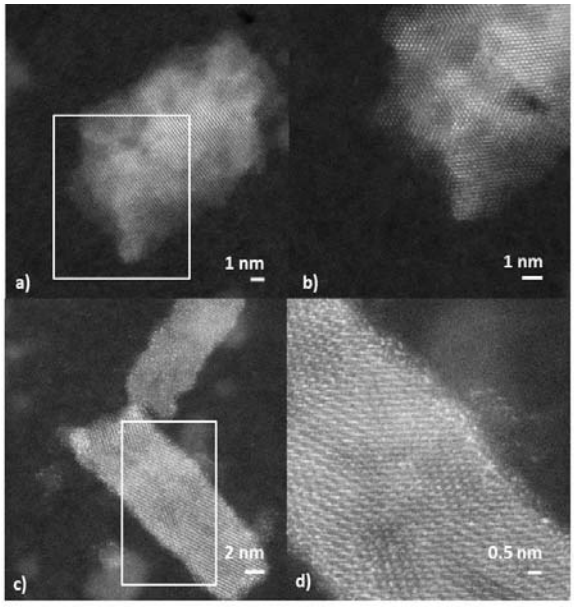

Fig. 4. High-resolution STEM micrographs of (a) TiO_2 nanoparticles showing the array of mesopores and c) REE-TiO_2 doped nanoparticles; (b, d) Magnifications of rectangular areas shown in (a) and (c) respectively

The labelling with La produced only a small increase of the specific surface area (from 239 to 246 m^2/g for the highest La concentration) while the Ce-labelled nanoparticles reached only 215 $m^2 \cdot g^{-1}$ (Table 2, Figure 3).

The porosity of TiO_2 nanoparticles could be also ascertained using high-resolution TEM, which showed an ordered array of mesopores on the surface of the nanoparticles obtained using this synthesis method (Figure 4). Further surface analysis using XPS showed spectral bands attributed to Ti, O, C and Ce or La elements (data not shown). A closer examination of the Ce3d or La3d signals around 900 eV and 850 eV, respectively, showed the doublet $3d_{5/2}$ and $3d_{3/2}$ lines (Figure 5), whose intensity increased as the content of the REE was increased during the

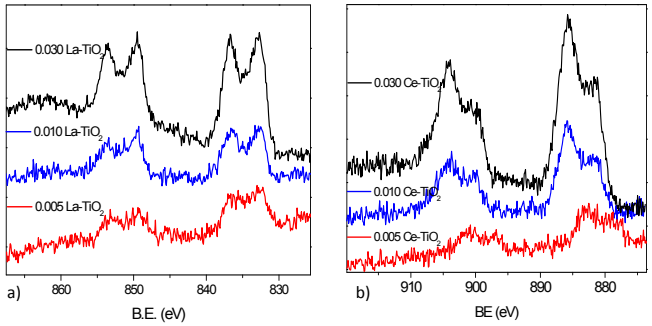

Fig. 5. XPS spectra of Ce3d and La3d bands of Ln-labelled TiO_2 nanomaterials

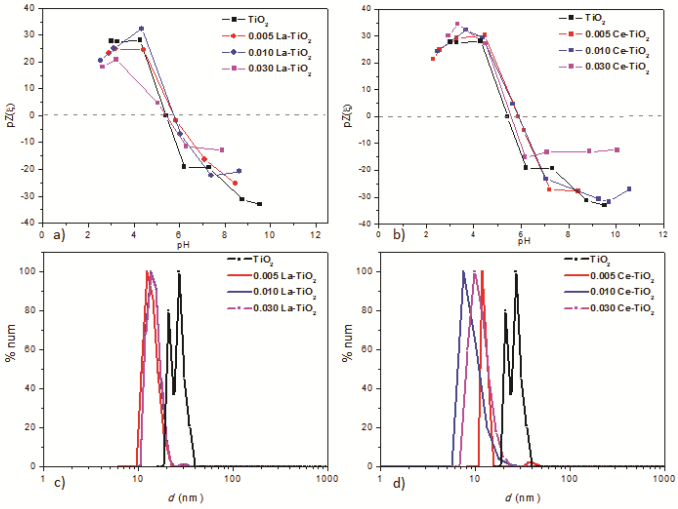

Fig. 6. Variation of the ζ-potential vs. pH (a, b) and hydrodynamic particle sizes measured from an pH 3 dispersion using DLS (c, d) of REE-labelled TiO_2 nanomaterials

synthesis. The REE/Ti atomic ratios were estimated from spectra of individual regions (Table 2), and their values were significantly higher than the ratios estimated from the proportions used during synthesis. This suggests a preferential concentration of lanthanide ions on the surfaces of individual particles or among the interfaces of the agglomerates, as it was reported elsewhere.[33] Other authors report that REE ions could occupy the interstitial octahedral sites in the anatase structure as it was reported for similarly doped TiO_2 nanomaterials with large

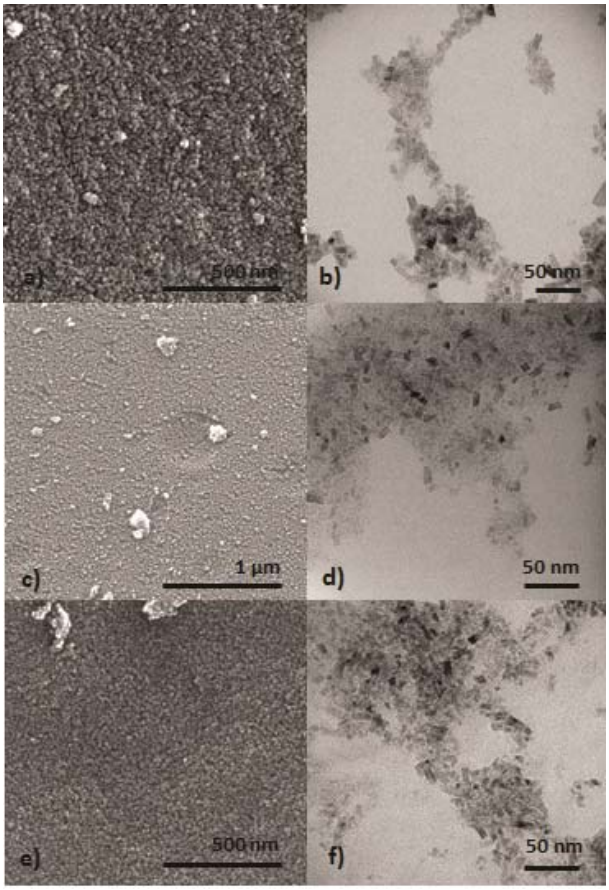

Fig. 7. SEM and TEM images of TiO_2 (a, b), 0.030 Ce-TiO_2 (c, d) and 0.030 La-TiO_2 (e, f). are given as insets

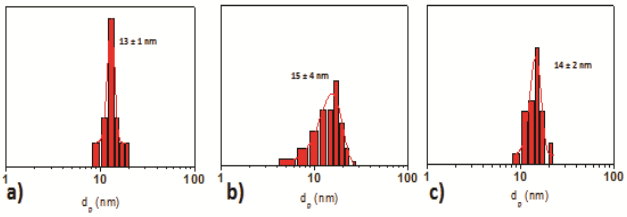

Fig. 8. Statistical size distribution (N > 75) of the nanoparticles observed in the TEM images of TiO_2 (a), 0.030 Ce-TiO_2 (b) and 0.030 La-TiO_2 (c).

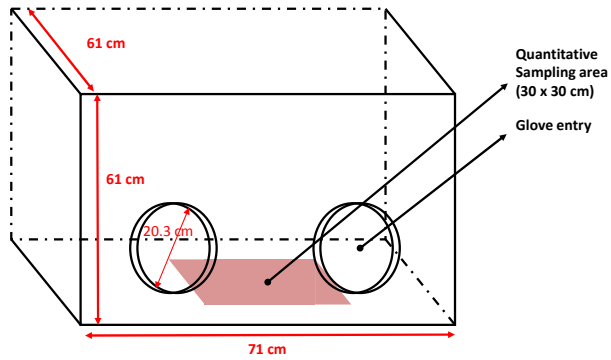

Fig. 9. Glove box and sampling area used for the quantitative analysis of surface deposition of labelled TiO_2 nanoparticles during handling

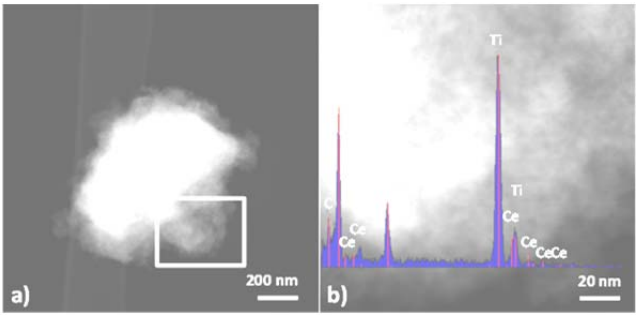

Fig. 10. (a) STEM dark-field images of the airborne matter collected by filtering the air around the manipulation area at 0.3 $L \cdot min^{-1}$ through a Cu grid during the manipulation of Ce-labelled TiO_2 nanoparticulate powders; (b) Magnification of rectangular area marked in (a), together with the EDX spectral analysis of the visualized area

contents of lanthanide ions (up to REE/Ti = 0.3.)[36]

Since the synthesis procedure combines a sol-gel processing followed by a fast microwave heating, mainly non-aggregated TiO_2 nanoparticles were obtained especially for the REE-doped material, as shown by DLS measurements. A narrow particle size distribution displayed can be observed for all the tested materials (Figure 6), with hydrodynamic particle sizes between 10-40 nm for REE-TiO_2 while it was slightly higher for TiO_2. The slightly lower hydrodynamic radius of the doped material could be due to a small change in the concentration of OH superficial groups due to the presence of Re-O-Ti bonds.[37] The surface charge of the REE-labelled nanoparticles was between -35 to 35 mV, with isoelectric points around pH 5, similar to that measured for TiO_2.

The electron microscopy analysis confirmed that REE-labelled TiO_2 nanoparticles display homogenous and regular shapes, similar to those found for unlabelled TiO_2 (Figure 7 and 8). Their prismatic shape is common for anatase nanostructures obtained using similar hydrothermal synthesis.[38] The sizes obtained from the TEM images for most of the primary particles of both undoped and REE-doped TiO_2 are in the 10-20 nm range.

Quantification of the surface deposition

To demonstrate the monitoring capabilities afforded by REE labelling a simple assessment of surface contamination by nanoparticles was attempted. To this end, nanoparticle deposition as a consequence of a simple powder manipulation process (transferring nanoparticles between two beakers) was studied in a controlled environment (glove chamber) to ensure the test repeatability and to avoid exposure (Figure 9).

The manipulation of Ce-labelled TiO_2 nanoparticles under such conditions led to a peak particle number concentration in the chamber after handling (Figure 1 SI).The airborne particles collected in the air around the sampling area formed agglomerates with sizes of a few hundred nm (Figure 10) and the STEM-EDX analysis confirmed the presence of cerium along with titanium in the collected particles (Figure 10b). This could confirm that the released matter could be effectively monitored using the cerium label in the TiO_2 nanoparticles. Similar results were obtained using La labelled nanoparticles (Figure 3 SI).

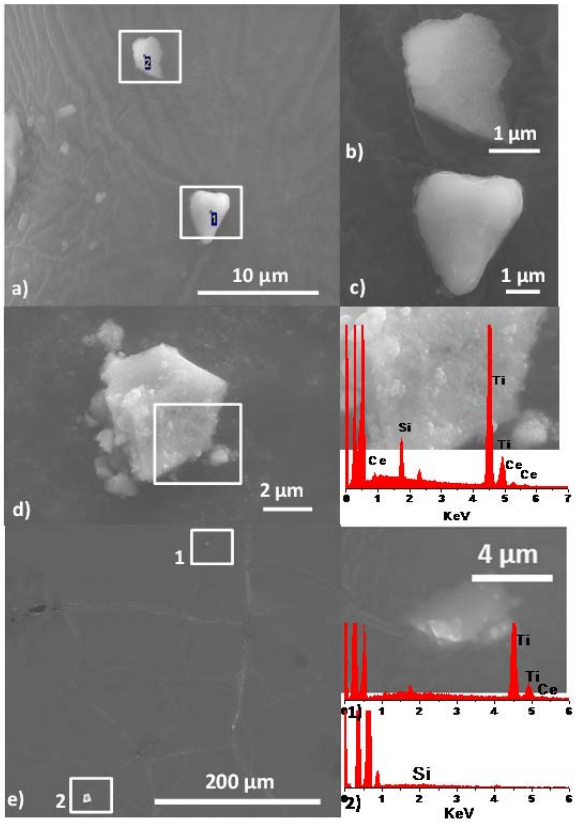

Fig. 11. (a) SEM image of particles settled on a carbon tape placed at 10 cm away from the source during the manipulation of TiO_2 nanoparticulate powders; (b, c) Magnification of areas marked with 2 and 1 in (a); (d) High magnification of a particle deposited on the carbon showing at right a close-up of the aggregates collected together with the EDX spectral analysis of the visualized area; (e) Survey SEM image to display the approximate distance between collected nanoparticles, showing at right a high magnification image of area marked with 1 in (e) (insets show the EDX spectral analysis of the areas marked as 1 and 2)

Particle agglomerates of a similar structure but with larger sizes (mean diameters below 10 µm) were found within a distance of 10 cm from the release point (Figure 11), which indicated that large aggregates were settled by gravitational forces on the testing area after manipulation. This strongly suggests the contamination of the working area by nanoparticle aggregates in the micron range. The fact that the contamination is in the form of aggregates rather than individual nanoparticles does not exclude toxicity, since nanoparticle aggregates still have a considerably higher surface area than bulk particles of the same size, and therefore the surface reactivity and cell toxicity are expected to be higher [39, 40].Therefore, Ce and La (see SI) labelling is effective in demonstrating surface contamination as a consequence of the handling of nanosized TiO_2 powders. Other elements (e.g. Si) could also be detected, which is attributed to the cross-contamination with the environmental airborne matter (Figure 11d and 11e). However, Ce or La are practically absent from environmental particles, and therefore they are effective as selective tags to identify objective nanomaterials.

Analytical determination of the deposited mass of nanoparticles

As we have shown, REE labelling is effective in discriminating individual nanoparticles and aggregates from those in the background. However, quantification of surface contamination by electron microscopy analysis of individual nanoparticles would be unpractical in terms of time and cost. Therefore we also attempted a quantitative estimation of surface contamination by chemical analysis of the REE labels after collecting and digesting the solid material deposited in the area under study.

The deposition of toxic metals in the surroundings of working areas has been analysed by a wiping procedure of the testing area, followed by a complete dissolution of the wipes together with the collected solid particles. The chemical analysis of such dissolution using flame-based optical spectrometry indicated the content of each REE label on the testing area.[41] This procedure is used by organizations such as the OSHA [42] in studies of exposure levels and threshold limit values for different metals. In our case, we have monitored the concentration of the lanthanide labels. A simple mass balance can then be used to quantify the contamination by nanoparticles in terms of mass of particle per unit of surface area. Lanthanides not only are absent from the unlabelled nanoparticles (and from most of the environmental material), but also very low limits of detection (LoD) can be achieved by common analytical techniques such as ICP-OES, allowing a sensitive estimation of surface contamination. Also, lanthanide atoms present spectra with numerous emission lines giving multiple opportunities to reduce potential interferences. In this work, the LOD obtained for Ce-labelled nanoparticles was as low as 0.0168 mg of Ce/L, when measuring at a wavelength of 413.4 nm. The capacity of this procedure for quantifying lanthanides was tested by spreading evenly a known amount or Ce-labelled TiO_2 nanoparticulate samples with a nominal Ce/Ti atomic ratio of 0.03 over a selected working area. The area was then subjected to the analytical wiping procedure described for metals and repeated three times (see Supporting Information for details). The results of the ICP-OES analysis of the digested wipes indicated that the Ce/Ti ratio of the deposited solid was 0.0269 ± 0.0022, slightly lower than that of the dispersed material, probably due to background contamination. The percentage of material recovered from the surface was 75 ± 6 %. The results obtained after pouring 500 mg of Ce-labelled TiO_2 powder between two beakers showed that the amount of nanoparticles deposited on the surface close to the operation was 0.14 ± 0.06 mg, corresponding to a surface contamination of 155.6 $\mu g \cdot cm^{-2}$ in the considered area of study.

Conclusions

Trace amounts of lanthanide ions could be easily incorporated into interstitial and surface sites of the anatase structure of TiO_2 nanoparticles. This procedure led to the synthesis of labelled TiO_2 nanoparticles with structures and properties similar to those of undoped nanoparticles. The use of lanthanides (Ce and La) as labels was selected in view of the negligible concentrations of these REE in background nanoparticles. Doping with Ce and La also favoured a high degree of sensitivity due to the low limits of detection found under testing conditions. This allowed the identification and quantification of the amount of deposited labelled matter onto working areas after common handling

operations. Consequently, this method could be effectively applied to determine the presence of labelled ENMs around working areas and therefore to reduce the potential exposure risks to engineered nanomaterials. In addition, the sensitivity of the method opens up possibilities of application for monitoring the release of nanosized matter in different industrial and environmental scenarios.

Notes and references

[a] *Department of Chemical Engineering, Nanoscience Institute of Aragon (INA), University of Zaragoza,50018 Zaragoza, Spain.*
[b] *Networking Research Center on Bioengineering, Biomaterials and Nanomedicine, CIBER-BBN, 50018 Zaragoza, Spain*

† Electronic Supplementary Information (ESI) available: [details of any supplementary information available should be included here]. See DOI: 10.1039/b000000x/

1. F. Balas, M. Arruebo, J. Urrutia and J. Santamaria, *Nat Nano*, 2010, **5**, 93-96.
2. P. Van Broekhuizen, W. Van Veelen, W.-H. Streekstra, P. Schulte and L. Reijnders, *Annals of Occupational Hygiene*, 2012, **56**, 515-524.
3. S. J. Klaine, P. J. J. Alvarez, G. E. Batley, T. F. Fernandes, R. D. Handy, D. Y. Lyon, S. Mahendra, M. J. McLaughlin and J. R. Lead, *Environmental Toxicology and Chemistry*, 2008, **27**, 1825-1851.
4. K. D. Grieger, I. Linkov, S. F. Hansen and A. Baun, *Nanotoxicology*, 2012, **6**, 196-212.
5. V. Gomez, S. Irusta, F. Balas and J. Santamaria, *J Hazard Mater*, 2013, **257**, 84-89.
6. R. D. Glover, J. M. Miller and J. E. Hutchison, *ACS Nano*, 2011, **5**, 8950-8957.
7. N. Lewinski, V. Colvin and R. Drezek, *Small*, 2008, **4**, 26-49.
8. A. D. Maynard, R. J. Aitken, T. Butz, V. Colvin, K. Donaldson, G. Oberdorster, M. A. Philbert, J. Ryan, A. Seaton, V. Stone, S. S. Tinkle, L. Tran, N. J. Walker and D. B. Warheit, *Nature*, 2006, **444**, 267-269.
9. W. Wohlleben, S. Brill, M. W. Meier, M. Mertler, G. Cox, S. Hirth, B. von Vacano, V. Strauss, S. Treumann, K. Wiench, L. Ma-Hock and R. Landsiedel, *Small*, 2011, **7**, 2384-2395.
10. D. Sekar, M. L. Falcioni, G. Barucca and G. Falcioni, *Environmental Toxicology*, 2014, **29**, 117-127.
11. H. Wang, L.-J. Du, Z.-M. Song and X.-X. Chen, *Nanomedicine*, 2013, **8**, 2007-2025.
12. A. D. Abid, D. S. Anderson, G. K. Das, L. S. Van Winkle and I. M. Kennedy, *Particle and Fibre Toxicology*, 2013, **10**.
13. N. Lubick, *Environmental Science & Technology*, 2009, **43**, 6446-6447.
14. M. Ono-Ogasawara, F. Serita and M. Takaya, *Journal of Nanoparticle Research*, 2009, **11**, 1651-1659.
15. T. M. Peters, S. Elzey, R. Johnson, H. Park, V. H. Grassian, T. Maher and P. O'Shaughnessy, *J Occup Environ Hyg*, 2009, **6**, 73-81.
16. P. Kumar, P. Fennell and A. Robins, *Journal of Nanoparticle Research*, 2010, **12**, 1523-1530.
17. K. Aschberger, C. Micheletti, B. Sokull-Klüttgen and F. M. Christensen, *Environment International*, 2011, **37**, 1143-1156.
18. T. Kuhlbusch, C. Asbach, H. Fissan, D. Göhler and M. Stintz, *Part Fibre Toxicol*, 2011, **8**, 22.
19. T. Dos Santos, J. Varela, I. Lynch, A. Salvati and K. A. Dawson, *Small*, 2011, **7**, 3341-3349.
20. C. Kirchner, T. Liedl, S. Kudera, T. Pellegrino, A. Muñoz Javier, H. E. Gaub, S. Stölzle, N. Fertig and W. J. Parak, *Nano Letters*, 2004, **5**, 331-338.
21. I. L. Medintz, H. T. Uyeda, E. R. Goldman and H. Mattoussi, *Nat Mater*, 2005, **4**, 435-446.
22. D. H. Oughton, T. Hertel-Aas, E. Pellicer, E. Mendoza and E. J. Joner, *Environmental Toxicology and Chemistry*, 2008, **27**, 1883-1887.
23. H. Hong, Y. Zhang, J. Sun and W. Cai, *Nano Today*, 2009, **4**, 399-413.
24. N. Gibson, U. Holzwarth, K. Abbas, F. Simonelli, J. Kozempel, I. Cydzik, G. Cotogno, A. Bulgheroni, D. Gilliland, J. Ponti, F. Franchini, P. Marmorato, H. Stamm, W. Kreyling, A. Wenk, M. Semmler-Behnke, S. Buono, L. Maciocco and N. Burgio, *Archives of Toxicology*, 2011, **85**, 751-773.
25. A. D. Dybowska, M.-N. Croteau, S. K. Misra, D. Berhanu, S. N. Luoma, P. Christian, P. O'Brien and E. Valsami-Jones, *Environmental Pollution*, 2011, **159**, 266-273.
26. F. Larner, Y. Dogra, A. Dybowska, J. Fabrega, B. Stolpe, L. J. Bridgestock, R. Goodhead, D. J. Weiss, J. Moger, J. R. Lead, E. Valsami-Jones, C. R. Tyler, T. S. Galloway and M. Rehkämper, *Environmental Science & Technology*, 2012, **46**, 12137-12145.
27. N. Neubauer, M. Seipenbusch and G. Kasper, *Annals of Occupational Hygiene*, 2013.
28. N. Neubauer, F. Weis, A. Binder, M. Seipenbusch and G. Kasper, *Journal of Physics: Conference Series*, 2011, **304**, 012011.
29. F. Gottschalk and B. Nowack, *Journal of Environmental Monitoring*, 2011, **13**, 1145-1155.
30. K. Abbas, I. Cydzik, R. Torchio, M. Farina, E. Forti, N. Gibson, U. Holzwarth, F. Simonelli and W. Kreyling, *Journal of Nanoparticle Research*, 2010, **12**, 2435-2443.
31. U. Holzwarth, A. Bulgheroni, N. Gibson, J. Kozempel, G. Cotogno, K. Abbas, F. Simonelli and I. Cydzik, *Journal of Nanoparticle Research*, 2012, **14**, 1-15.
32. V. Gomez, S. Irusta, F. Balas, N. Navascues and J. Santamaria, *Journal of Hazardous Materials*.
33. V. Gomez, A. M. Balu, J. C. Serrano-Ruiz, S. Irusta, D. D. Dionysiou, R. Luque and J. Santamaría, *Applied Catalysis A: General*, 2012, p. 47-53.
34. V. Štengl, S. Bakardjieva and N. Murafa, *Materials Chemistry and Physics*, 2009, **114**, 217-226.
35. M. Fernández-García, X. Wang, C. Belver, J. C. Hanson and J. A. Rodriguez, *The Journal of Physical Chemistry C*, 2006, **111**, 674-682.
36. J. Xu, Y. Ao, D. Fu and C. Yuan, *Colloids and Surfaces A: Physicochemical and Engineering Aspects*, 2009, **334**, 107-111.
37. J. Reszczyńska, T. Grzyb, J. W. Sobczak, W. Lisowski, M. Gazda, B. Ohtani and A. Zaleska, *Applied Surface Science*, 2014, **307**, 333-345.

38. Sawanta S. Mali, Hyungjin Kim, Chang Su Shim, Pramod S. Patil, Jin Hyeok Kim, and and C. K. Hong, *Scientific reports*, 2013, **3**.
39. R. I. M. Justin M. Zook, Laurie E. Locascio, Melissa D. Halter & John T. Elliott, *Nanotoxicology*, 2011, **5**, 517-530.
40. A. Albanese and W. C. W. Chan, *ACS Nano*, 2011, **5**, 5478-5489.
41. K. Ashley, G. Braybrooke, S. D. Jahn, M. J. Brisson and K. T. White, *J Occup Environ Hyg*, 2009, **6**, 15459620903022597.
42. K. Ashley, T. J. Wise, D. Marlow, A. Agrawal, J. P. Cronin, L. Adams, E. Ashley and P. A. Lee, *Analytical Methods*, 2011, **3**, 1906-1909.